Environ Monit Assess (2023) 195:682
https://doi.org/10.1007/s10661-023-11247-0

RESEARCH

Dynamic removal of Pb(II) by live *Dunaliella salina*: a competitive uptake and isotherm model study

Somayyeh Ziaei · Hossein Ahmadzadeh · Zarrin Es'haghi

Received: 23 November 2022 / Accepted: 13 April 2023

Abstract The main aim of this study is modeling of a continuous biosorption system for the removal of Pb(II) ions in the aqueous conditions using live *Dunaliella salina* microalgae. The live microalgae can grow in saline water and opens new opportunities in varying the amount and properties of biosorbent. The effects of five parameters, including pH, optical density of algae as a factor indicating the adsorbent dosage, injection time, contact time, and initial concentration of Pb(II), were optimized by means of response surface methodology (RSM) based on the central composite design (CCD). *Dunaliella salina* algae showed maximum Pb(II) biosorption with 96% efficiency. For the selective Pb(II) uptake in the presence of Cd(II) and Ni(II), binary and ternary systems of ions were chosen. The mutual effect of each heavy metal ion in all systems on the total uptake percentage was also examined. The ion selectivity was investigated in the presence of diverse heavy metal ions, and the Pb(II) uptake percentage was determined to be 80%. Both Langmuir and Freundlich isotherm models were suitable for describing multicomponent binary and ternary systems depending on the presence of competitive ions in the mixture. Main functional groups and surface properties of the *Dunaliella salina* were identified by Fourier transform infrared spectroscopy, scanning electron microscopy, and energy dispersive spectrometry. Hence, effective heavy metal ion uptake, simple design, and cost-effective cultivation confirmed live *Dunaliella salina* as suitable microalgae for purifying contaminated water in an economic and safe manner.

Keywords Biosorption · Heavy metal ions · *Dunaliella salina* · Response surface methodology

Introduction

The environmental pollution of heavy metal ions due to industrial developments such as mining, tannery, photography, petroleum refining, pesticides, and metallurgical and manufacturing activities have become a major global concern. These activities have led to the release of various amounts of toxic metal ions in the food chain of living creatures due to waste disposal in their ecosystem (Vidyalaxmi et al., 2019). Heavy metal ions are non-biodegradable even at low concentrations. Hence, their persistence has become a global issue in many countries because of their capacity for bioaccumulation in human and animal tissues by exposure to water or food derived from natural water (Wei et al., 2021; Ziaei et al., 2022).

Pb(II), Cd(II), and Ni(II) as heavy metal ions are used in a wide range of commercial procedures (Esvandi et al., 2019). For example, Pb(II) can damage the brain and

Supplementary Information The online version contains supplementary material available at https://doi.org/10.1007/s10661-023-11247-0.

S. Ziaei · H. Ahmadzadeh (✉)
Department of Chemistry, Faculty of Science, Ferdowsi University of Mashhad, Mashhad 9177948974, Iran
e-mail: h.ahmadzadeh@um.ac.ir

Z. Es'haghi
Department of Chemistry, Payame Noor University, Tehran 19395-4697, Iran

Published online: 16 May 2023

central nervous system (Eliescu et al., 2020). Cd(II) can be found in many products such as batteries, paints, and plastics. It can cause damage to the lining of the lungs, liver, and kidneys, as well as cancer and the destruction of red blood cells (Abdel et al., 2013; Verma et al., 2021). Also, Ni(II), at over-permissible levels, causes kidney damage, lung cancer, and gastrointestinal disorder (Giraldo et al., 2019). Therefore, the elimination of heavy metal ions at an acceptable level is considered a major issue due to the economic and environmental concerns. To reduce these effects, many traditional methods consisting of chemical or electrochemical precipitation, ion exchange systems, membrane separation process, advanced oxidation, coagulation, reverse osmosis, electro dialysis, and solidification have been developed and established to remove heavy metal ions from wastewaters (Gu et al., 2021; Zhang et al., 2022; Zhang et al., 2020). Unfortunately, the application of these methods has been limited by some factors such as ineffective performance, deficiency of eco-friendliness, and maintenance costs that make them unattractive and unsatisfactory in wastewater treatment (Anastopoulos & Kyzas, 2015; Qin et al., 2020; Wang & Chen, 2009).

In comparison to conventional techniques, numerous studies on various biological adsorption methods are considered suitable for the treatment of contaminated waters (Kamal & Rafey, 2021; Katheresan et al., 2018; Morosanu et al., 2017). Biosorption by natural materials is considered as an innovative and cost-effective method (Pugazhendhi et al., 2018; Qin et al., 2020).Various natural biosorbents such as rice straw (Shen et al., 2019), fungal biomass (Kumar et al., 2008), cucumber peel (Basu et al., 2017), fruit peels (Turkmen Koc et al., 2020), and yeast (Wang & Chen, 2009) have been examined to eliminate heavy metal ions. Recently, one of the most promising biosorbents introduced is the algal species (Elleuch et al., 2021; Mohd Udaiyappan et al., 2017). Algae are primary organisms in the biological systems widely spread around the world. Algae cell walls are surrounded by polysaccharides, proteins, and lipid matrix that provide facilitating functional groups to bind heavy metal ions (Gu & Lan, 2021; Naveed et al., 2019; Suresh Kumar et al., 2015; Yan et al., 2022). Several studies have been reported on biological metal ion removal, including Cu(II), Pb(II), Co(II), Fe(II), Cr(III), As(III), and Ni(II) ions and organic dyes by various algae species (Bai & Venkateswarlu, 2019; Fawzy & Gomaa, 2020; Fawzy et al., 2020; Giraldo et al., 2019; Lee & Chang, 2011). Different mechanisms such as electrostatic attraction, cation exchange, formation of metal complexes, hydrogen bond formation, and microprecipitation can occur in the biosorption process (Fawzy & Gomaa, 2020; Giraldo et al., 2019). Hence, the biosorption capacity relies on the algal species and charges on metal ions (Dönmez & Aksu, 2002; Zeraatkar et al., 2016). *Dunaliella salina (D. salina)* is one type of green microalgae with a very high capacity for binding metal ions due to the presence of functional groups such as amines, hydroxyls, carboxyl, and sulfates, which can cross-link with heavy metal ions depending on temperature, concentration of heavy metal ions, and pH (Wang et al., 2017). Moreover, researchers confirmed that *D. salina* requires minimal nutrients and environmental conditions (Anastopoulos & Kyzas, 2015) and can survive even in harsh natural conditions.

Most reports on using microalgae for the biosorption of heavy metal ions use biomass as the biosorbent. The use of biomass is straightforward and simple, but using live microalgae is very challenging. So far, there are few reports on using live microalgae as a continuously growing biosorbent (Suresh Kumar et al., 2015). The growth curve of live microalgae shows the complexity of the production of biosorbents in different stages of the growth kinetics. Most models for sorption and biosorption using biomass rely on simple mathematics of a constant amount of biosorbent being added to the solution at the beginning of the process. When using live microalgae, due to the constant production of biosorbent at different rates, most of the classical models fail to explain the process. The aim of the current research is to investigate the efficiency of live *D. salina* algae as an environment-friendly and economical biosorbent for wastewater treatment in a dynamic process. This microalgae has a high growth rate in saline water and can produce harvestable biomass. Several studies have been introduced to use *D. salina* biomass as an effective metal ion biosorbent from wastewater (Belghith et al., 2016; Elleuch et al., 2021). On the contrary of previous reports, the present research uses a singular step of growing algae directly to remove heavy metal ions through a continuous sorption system of contaminated water. In particular, no previous report is seen on continuous sorption of Pb(II) by living *D. salina*, mechanism, and measuring the time of feeding contaminated water, which is an effective parameter in the growth process.

Additionally, industrial wastes often include multicomponent heavy metal ions. The assessment of only

one type of metal ion uptake may not be acceptable (Plazinski, 2013). Based on the literature, no report was found on simultaneous Pb(II), Cd(II), and Ni(II) uptake using live *D. salina*. In order to more precisely understand the interactions between the competitive heavy metal ions and environmental complications, the biosorption of heavy metal ions in single, binary, and ternary solutions was investigated.

In this work, the influence of several important factors such as pH, contact time, optical density (OD) as adsorbent dosage, injection time of Pb(II), and initial concentration of Pb(II) are investigated by response surface methodology (RSM). Out of several designs available for optimization, the RSM design was chosen as the most efficient design, with less time and fewer test runs for Pb(II) uptake (Isam et al., 2019). *D. salina* surface also was characterized by means of scanning electron microscopy (SEM) and energy dispersive spectrometry (EDS). Also, to identify the main functional groups for the interaction of algae and heavy metal ions, Fourier transform infrared (FT-IR) spectroscopy was used (Lee & Chang, 2011). Hence, this study recommends an effective and dynamic method to use live *D. salina* for the purification of water from heavy metal ions at a low cost.

Materials and methods

Chemical materials

Pb $(NO_3)_2$ (purity > 99%, Merck), Cd $(NO_3)_2{\cdot}4H_2O$ (purity > 99%, Fluka), and Ni $(NO_3)_2{\cdot}6H_2O$ (purity > 99%, Sigma-Aldrich) were used in stock solutions. Sodium hydroxide (0.1 mol L^{-1}) and nitric acid (1%) solutions were prepared for pH adjustment (Riedel-de-Haen, Germany). All the stock solutions were prepared using deionized (DI) water. All chemical reagents used were of analytical grade without further purification.

Analytical procedures

The concentration of Pb(II), Cd(II), and Ni(II) in the solution was determined using an atomic absorption spectrophotometer (AAS) (Analytik Jena AG, 07,745 Jena, Germany). The surface morphological features of the *D. salina* before and after the removal of heavy metal ions were analyzed using SEM and EDX (TESCAN-XMU, Czech Republic). FT-IR spectrometry (Thermo Nicolet Avatar 370, Pittsfield, USA) was used to determine the functional groups of the *D. salina* surface. The ion selectivity was studied using inductively coupled plasma-optical emission spectrometry (ICP-OES) (76004555 SPECTRO ARCOS System).

D. salina microalgae growth conditions

The stock microalgae *D. salina* was cultured in a 300.0-mL Erlenmeyer flask containing 250 mL artificial seawater (ASW) with the following composition (g L^{-1}) (Kester et al., 1967): NaCl 23.6, $MgCl_2.6H_2O$ 4.1, $MgSO_4.7H_2O$ 4.9, $CaCl_2$ 1.1, KNO_3 0.3, KCl 0.075, Na_2EDTA 0.012, $Na_2SiO_3.9H_2O$ 0.04, enriched with 1.0 mL of trace element stock with the following composition (g L^{-1}): H_3BO_3 0.57, $MnCl_2.4H_2O$ 0.36, $ZnCl_2$ 0.62, $CuCl_2.2H_2O$ 0.27, $Na_2MoO_4.2H_2O$ 0.25, $CoCl_2.6H_2O$ 0.42, $FeSO_4$ 1.36, $MnCl_2.4H_2O$ 0.36, $Na_2C_4H_4O_6$ 1.77, and 10.0 mL KH_2PO_4 4.6 (g L^{-1}). This solution was sterilized by autoclaving at 120 °C for 2 h. The initial growth medium pH was 6.4. The culture was maintained under continuous fluorescent lamps with 50 µmol m^{-2} s^{-1}light intensity with 16–8 h light–dark cycle at 25 ± 2 °C and for 14 days.

To determine the algae growth curve, the turbidity of *D. salina* culture was measured at 680 nm daily using a spectrophotometer, and the algae growth curve is shown in Fig. 1. Then, stock *D. salina* was placed in a refrigerator, and sub-cultures were prepared from this solution. All experiments were conducted in triplicates, and data were expressed as mean values with standard deviations to minimize error.

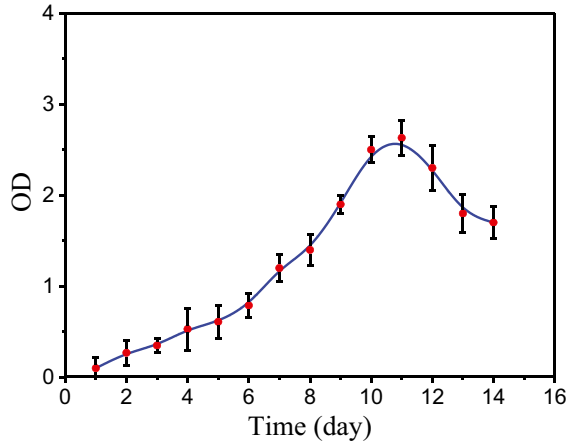

Fig. 1 Growth curve of *D. salina*

Sorption experiments

The metal ion stock solutions of $Cd(NO_3)_2$, $Pb(NO_3)_2$, and $Ni(NO_3)_2$ were prepared in a 100-mL volumetric flask at the concentration of 1000 (mg L^{-1}) in deionized water. All necessary solutions were diluted from the stock solutions.

The effects of several parameters, including initial Pb(II) concentration, pH, OD, injection time of Pb(II), and contact time, on the Pb(II) uptake using *D. salina* were investigated. The flasks of algal culture were prepared according to the *D. salina* microalgae growth condition section. After the end of biosorption, the algae samples were centrifuged at 5000 rpm to separate the biosorbent. For pH adjustment, a small amount of HNO_3 (1%) or NaOH (0.1 mol L^{-1}) was used. The growth media pH of *D. salina* decreases from 6.4 due to the interaction between pH and dissolved CO_2. To study the effect of growth media pH on Pb(II) uptake, the pH was changed to 3, 4, 5, 6, and 7 at a different growth rate of *D. salina.* The optimum conditions for Pb(II) uptake were selected using these experiments.

To study the influence of heavy metal ions on biosorption and total uptake, Pb(II), Cd(II), and Ni(II) with a concentration range of 0–300.0 mg L^{-1} were examined. For binary systems, six experimental sections were designed as follows: the concentration of Cd(II) and Ni(II) were individually varied from 0 to 300.0 mg L^{-1} in the presence of Pb(II) (50.0 mg L^{-1}). The concentration of Pb(II) and Ni(II) was individually changed from 0 to 300.0 mg L^{-1} in the presence of 50.0 mg L^{-1} of Cd(II). The concentration of Pb(II) and Cd(II) was individually changed from 0 to 300.0 mg L^{-1} in the presence of 50.0 mg L^{-1} of Ni(II). For ternary biosorption, one experimental section was designed: the concentration of Cd(II) and Ni(II) was simultaneously changed from 0 to 300.0 mg L^{-1} in the presence of 50.0 mg L^{-1} of Pb(II).

Design of experiments

Response surface methodology with a central composite design (RSM-CCD) approach was utilized to design and optimize the biosorption tests. Simultaneously, the effects of five parameters were determined, including: pH (A), OD (B), initial Pb(II) concentration (C), injection time of Pb(II) (D), and contact time (E). Table 1 shows the coded levels and lower and higher ranges for each selected parameter.

Thirty-two experiments were recommended by CCD design. Pb(II) uptake was considered as the response. In this study, half factorial CCD was applied. The CCD for the five independent parameters was based on ten axial points, sixteen factorial points, and six replicates as the center point. The selected parameters were varied at five levels labeled as: $(-\alpha, -1, 0, +1,$ and $+\alpha)$. The number of experiments was obtained using Eq. (1):

$$N_e = \frac{2^P}{2} + 2P + C.P \quad (1)$$

N_e is the number of experiments, P is the number of independent parameters, and C.P is the number of experiments conducted at the center point. A set of the 32-experiment matrices was obtained, as shown in Experimental design and statistical analysis section. To minimize systematic bias, the experiments were carried out in a randomized design. The experimental data matrix was employed using Minitab, 17.0.1, and Design-Expert, 12.

Statistical methods

The analysis of variance (ANOVA) and three-dimensional (3D) surface plots were obtained to evaluate the statistical significance and the interaction between the selected parameters for Pb(II) biosorption. In

Table 1 Levels of independent parameters based on CCD method for Pb(II) uptake%

Parameters	Unites	Symbols	Levels				
			$-\alpha$	-1	0	$+1$	$+\alpha$
pH	-	A	3	4	5	6	7
OD	-	B	0.1	0.2	0.3	0.4	0.5
Pb(II) concentration	mg L^{-1}	C	10	82.5	155	227.5	300
Injection time	day	D	2	4	6	8	10
Contact time	h	E	24	36	48	60	72

addition, the regression model (R^2) was explained to describe the correlation between variables and the response function.

Biosorption isotherms and data evaluation

The biosorption isotherms with the initial concentration range of 50.0–300.0 mg L^{-1} for Cd(II), Ni(II), and Pb(II) were investigated under optimal conditions. The final heavy metal ion concentrations were analyzed using AAS. The individual and total uptake of heavy metal ions was calculated using Eqs. (2) and (3), respectively:

$$\%\, M(II)\ uptake = \frac{\left(C_i - C_f\right)}{C_i} \times 100 \tag{2}$$

$$\%\ Total\ uptake = \frac{\sum \left(C_i - C_f\right)}{\sum C_i} \times 100 \tag{3}$$

The biosorption capacity q_e (mg g^{-1}) was obtained to determine the Langmuir and Freundlich models according to the following equation:

$$q_e = \frac{\left(C_i - C_f\right)V}{m} \tag{4}$$

In Eqs. (2) to (4), C_i (mg L^{-1}) and C_f (mg L^{-1}) represent the initial and final concentrations of heavy metal ions, respectively, V (L) is the volume of algae sample, and m(g) is the mass of biosorbent dosage (*D. salina*).

Real sample assessment

In order to observe the behavior of *D. salina* for heavy metal ion uptake in real samples, two experiments using real water spiked with Pb(II), Cd(II), and Ni(II) were performed. The real saline water samples were obtained from the Caspian Sea and well water. *D. salina* was grown at the volume of 100 mL of real samples, and heavy metal ions were spiked with 50.0 mg L^{-1} of Pb(II), Cd(II), and Ni(II) ions.

Results and discussion

Experimental design and statistical analysis

The effects of five independent variables, including: pH (A), OD(B), initial Pb(II) concentration (C), injection time of Pb(II) (D), and contact time (E) on biosorption were carried out with RSM-CCD to obtain the optimum conditions. The CCD proposed matrix of input parameters and Pb(II) uptake with the 32 randomized experiments is designed in Table 2. Based on the mathematical relationship among variables and response function using RSM, the coefficients of the equation and quadratic model for Pb(II) uptake is shown in Eq. (5):

$$\begin{aligned} Pb(II)\ uptake\ \% \ =\ & +\ 86.79\ +\ 0.8097A\ +\ 0.2923B\ -\ 3.44C\ +\ 0.3197D \\ & +\ 0.2983E\ +\ 0.0778A^2\ +\ 0.6203B^2\ +\ 0.4678C^2 \\ & -\ 0.3059D^2\ -\ 0.0313E^2\ +\ 0.0809AB\ +\ 0.1904AC \\ & +\ 1.21AD\ +\ 0.3516AE\ -\ 0.4234BC\ -\ 0.2279BD \\ & -\ 0.2521BE\ -\ 1.10CD\ -\ 0.6866CE\ -\ 0.5146DE \end{aligned} \tag{5}$$

A, B, C, D, and E are the coded values for the selected variables, while AB, AC, AD, AE, BC, BD, BE, CD, CE, and DE are the interaction parameters. The quadratic terms are A^2, B^2, C^2, D^2, and E^2. The analysis of variance (ANOVA) for Pb(II) (II) uptake is given in Table 3, which consists of F-value, p-value, lack of fit, and pure error.

In general, if the p-value in the ANOVA is less than 0.05, the variables are significant (Mosleh et al., 2018; Sohbatzadeh et al., 2016). According to the ANOVA results in Table 3, A, C, AD, CD, CE, DE, B^2, and C^2 are significant model terms. The F-value of 29.80 implies that the model is significant. There is only a 0.01% chance that an F-value this large could occur due to noise. The coefficient of determination, R^2 value, for Eq. (5) and the standard deviation of the model are 0.9819 and 0.8078, respectively (Table 4).

The regression model is an appropriate way to describe the correlation between variables and the response function. The closer R^2 is to 1 and smaller the standard deviation implied that the model is significant and could establish a suitable relationship between the variables and Pb(II) uptake. Moreover,

Table 2 Designed runs for Pb(II) uptake using *D. salina*

Run	*A*: pH	*B*: OD	C: Pb(II)	*D*: injection time	*E*: contact time	Pb(II) uptake
			mg L^{-1}	day	h	%
1	4	0.2	227.5	8	60	80.60
2	4	0.4	227.5	8	36	82.21
3	4	0.4	227.5	4	60	84.96
4	6	0.2	227.5	4	60	85.32
5	6	0.2	82.5	8	60	94.36
6	5	0.3	155	6	48	80.00
7	5	0.3	155	6	48	86.42
8	4	0.4	82.5	8	60	90.72
9	5	0.3	155	10	48	88.93
10	6	0.4	82.5	8	36	93.83
11	5	0.3	10	6	48	96.32
12	4	0.2	82.5	4	60	90.70
13	5	0.5	155	6	48	90.00
14	5	0.3	155	6	72	87.37
15	5	0.3	155	6	48	87.68
16	3	0.3	155	6	48	85.44
17	5	0.3	155	2	48	84.79
18	4	0.4	82.5	4	36	90.11
19	6	0.4	82.5	4	60	91.52
20	6	0.4	227.5	8	60	84.40
21	6	0.4	227.5	4	36	84.70
22	6	0.2	82.5	4	36	85.60
23	5	0.1	155	6	48	89.13
24	5	0.3	300	6	48	81.58
25	5	0.3	155	6	48	85.89
26	4	0.2	82.5	8	36	89.50
27	5	0.3	155	6	48	86.24
28	4	0.2	227.5	4	36	85.21
29	5	0.3	155	6	48	85.95
30	7	0.3	155	6	48	89.35
31	5	0.3	155	6	24	86.55
32	6	0.2	227.5	8	36	85.89

the *F*-value of 0.6049 for lack of fit implies that lack of fit is not significant relative to the pure error. This result demonstrated that lack of fit is good. The other numerical parameters of this model are summarized in Table 4.

Furthermore, adequate precision, which measured the signal-to-noise ratio (S/N), was 22.7752. A ratio (S/N) greater than 4 is desirable and shows a suitable signal. This model can be utilized to navigate the design space (Isam et al., 2019). Based on the *F*-value results of independent parameters, the main effects of independent parameters on Pb(II) uptake followed this sequence: initial concentration of Pb(II) > pH > injection time > contact time > OD. Based on the results in Table 3, this model was significantly affected by the two first orders of independent parameters, including pH and initial Pb(II)concentration (p-value < 0.05). The OD, contact time, and injection time had a little effect on the Pb(II) uptake. Therefore, they are identified as insignificant factors (p-value > 0.05).

Table 3 ANOVA table for Pb(II) uptake using *D. salina* microalgae

Source	Sum of squares	DF	Mean square	*F*-value	*p*-value
Model	388.96	20	19.45	29.80	< 0.0001
A	15.74	1	15.74	24.12	0.0005
B	2.05	1	2.05	3.14	0.1040
C	283.69	1	283.69	434.74	< 0.0001
D	2.45	1	2.45	3.76	0.0786
E	2.14	1	2.14	3.27	0.0978
AB	0.1047	1	0.1047	0.1604	0.6965
AC	0.5799	1	0.5799	0.8886	0.3661
AD	23.27	1	23.27	35.65	< 0.0001
AE	1.98	1	1.98	3.03	0.1095
BC	2.87	1	2.87	4.39	0.0600
BD	0.8308	1	0.8308	1.27	0.2832
BE	1.02	1	1.02	1.56	0.2378
CD	19.30	1	19.30	29.58	0.0002
CE	7.54	1	7.54	11.56	0.0059
DE	4.24	1	4.24	6.49	0.0271
A^2	0.1778	1	0.1778	0.2724	0.6121
B^2	11.29	1	11.29	17.30	0.0016
C^2	6.42	1	6.42	9.84	0.0095
D^2	2.74	1	2.74	4.21	0.0649
E^2	0.0288	1	0.0288	0.0441	0.8375
Residual	7.18	11	0.6526		
Lack of fit	3.02	6	0.5032	0.6049	0.7220
Pure error	4.16	5	0.8318		
Cor. total	396.14	31			

Effect of process parameters on the Pb(II) uptake

Three-dimensional (3D) surface plots were used to assess the interaction behavior of two parameters (horizontal plane) on the Pb(II) uptake (vertical axis), while the other three parameters are kept at fixed levels (Fig. 2a–j). pH is one of the essential parameters that seriously affects biosorption (Esposito et al., 2002). The interaction of pH with OD, Pb(II) concentration, injection time, and contact time on Pb(II) uptake is depicted in Fig. 2a–d, respectively. As shown in Fig. 2b, interaction of Pb(II) concentration and pH indicates a significant response to Pb(II) uptake. The adsorption efficiency increased with increase in solution pH. At high pH, the surface of the algae is negative and causes more affinity interactions with Pb(II) (Kit & Chang, 2020). Also, for effective biosorption, the pH of the algae surface should be higher than the point of zero charge (pH_{PZC}) (Fawzy et al., 2022). If the pH value is lower than the pH_{pzc}, the algae surfaces would be protonated, and the biosorption of heavy metal ions will decrease. In addition, H^+ ions may compete with Pb(II) species. At pH > 7, precipitation would occur, and Pb(II) uptake will not be feasible. The optimum pH value for Pb(II) bisorption was 6, and the final pH value after Pb(II) biosorption was measured to be 4.8.

Also, it was observed that uptake efficiency was reduced by increasing the Pb(II) concentration. This behavior might be due to the saturation of active functional groups existing on the *D. salina* surface at a high concentration of Pb(II) (Kit & Chang, 2020). Interestingly, as shown in Fig. 2h, the Pb(II) uptake percentage was increased by increasing the injection time of Pb(II) from days 2 to 10 in growing process of algae. This important result confirmed that growing rate of *D. salina* was due to increasing microalgae as fresh biosorbent with new binding sites on its surface.

Table 4 Statistical variables from (CCD-RSM)

No.	Parameter	Pb(II) uptake
1	Standard deviation	0.8078
2	Mean	87.42
3	C.V. %	0.9241
4	R^2	0.9819
5	Adjusted R^2	0.9489
6	Predicted R^2	0.7931
7	Adequate precision	22.7752

Single, binary, and ternary biosorption processes

In order to investigate the effect of competitive ions on heavy metal ion uptake efficiency, seven experimental sections (A–G) were carried out. Table 5 shows the heavy metal ion uptake by *D. salina* in the single, binary, and ternary systems. Generally, in multicomponent biosorption process, three types of behaviors may occur: 1. Synergism phenomenon can occur leading to increasing the total uptake in the presence of other heavy metal ions; 2. Antagonism behavior happens due to decrease in the total uptake in the presence of other heavy metal ions, and. 3. Non-interaction may happen (Verma et al., 2021). The simultaneous Cd(II), Ni(II), and Pb(II) uptake from binary heavy metal ion solutions were examined in sections A–D. In sections A and B, initial Pb(II) concentration was fixed (50.0 mg L^{-1}), while Cd(II) and Ni(II), as competitive ions, were increased (0–300.0 mg L^{-1}). It was observed that the Pb(II) uptake % decreased from 96.19 to 80.99 and from

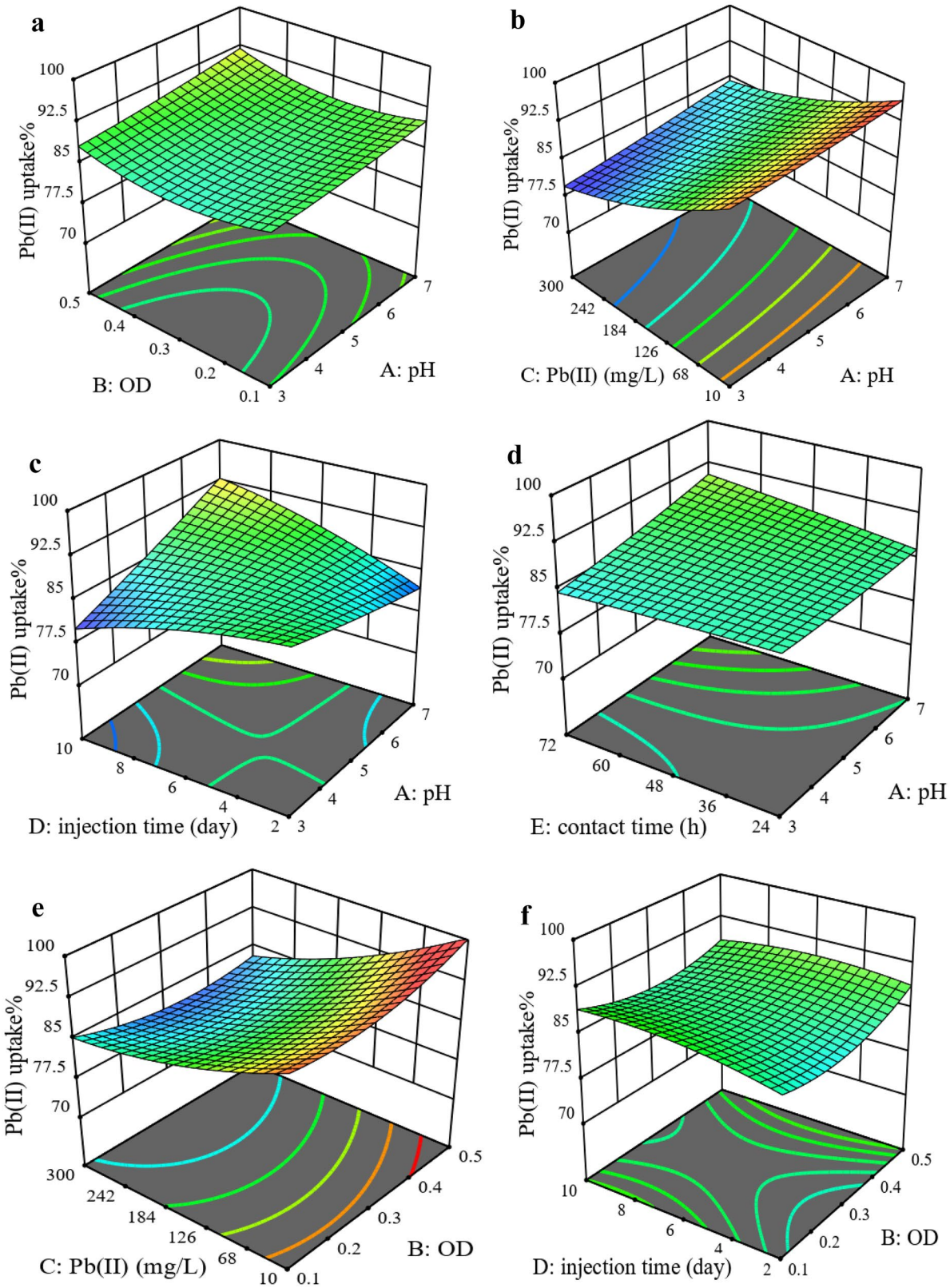

Fig. 2 (3D-RSM) plots for Pb(II) uptake versus effect of parameters

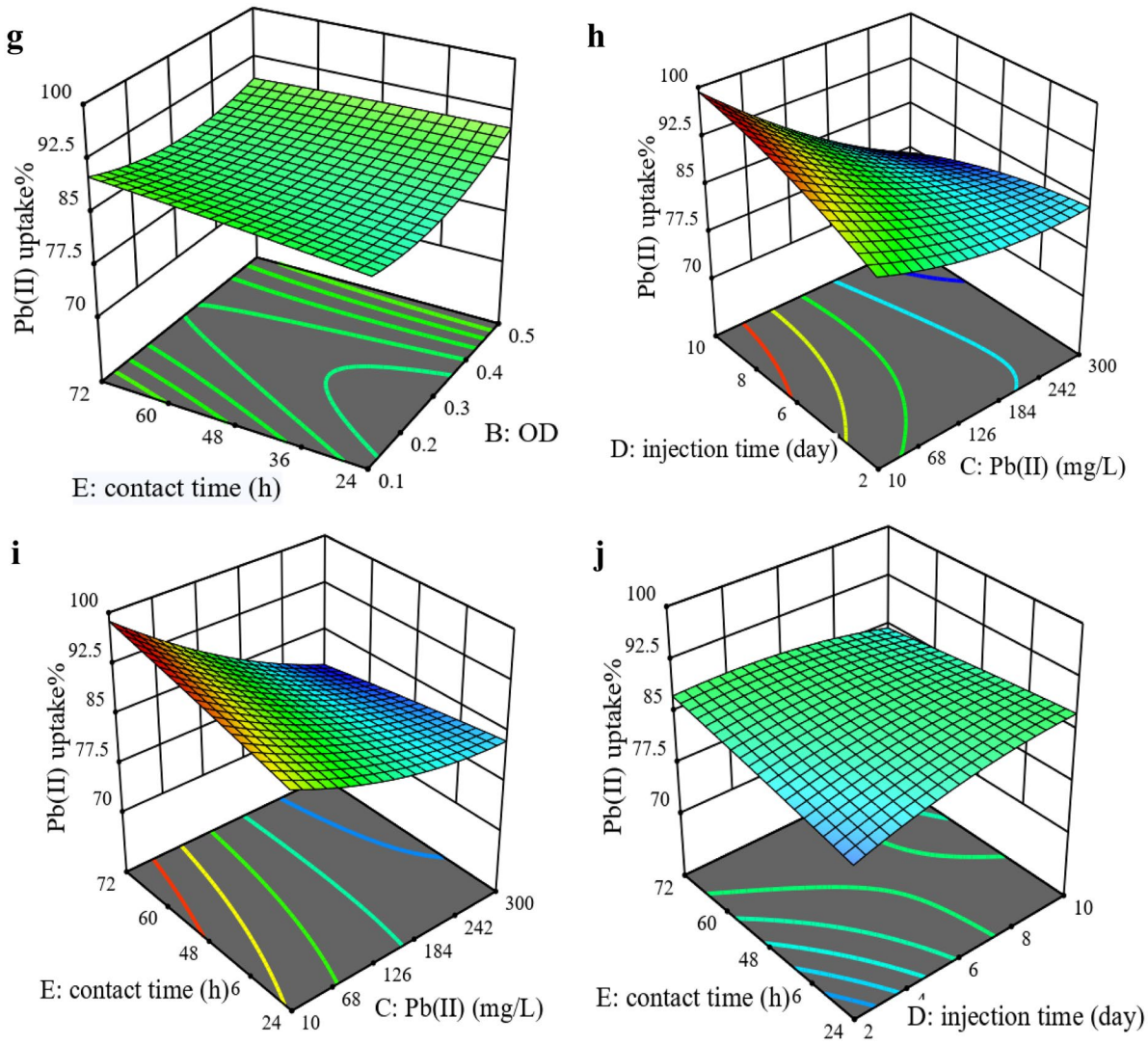

Fig. 2 (continued)

96.19 to 95.51 with increase in the initial concentration of Cd(II) and Ni(II), respectively. Also, Cd(II) and Ni(II) uptake percentages were decreased as compared to single metal ion uptake. This phenomenon shows a competitive effect among Cd(II), Ni(II), and Pb(II) ions. However, Pb(II) uptake is higher than Cd(II) and Ni(II) uptake. A similar pattern was observed for Ni(II) in the presence of Pb(II) in section B. But the amount of Ni(II) uptake (35.63–10.80%) was lower as compared to Cd(II) uptake (76.22–22.00%). It was noticed that with increasing competitive ion concentration, the Pb(II)uptake% was reduced. Therefore, the antagonistic effect occurred in the presence of Cd(II) and Ni(II) on the Pb(II) uptake.

In sections C and D, the concentration of Cd(II)and Ni(II) ions were fixed (50.0 mg L^{-1}), and Pb(II) was increased from 0 to 300.0 mg L^{-1}. As shown in these sections, Pb(II) uptake was higher than Cd(II) and Ni(II) uptake percentages. Cd(II) and Ni(II) uptake was similarly decreased. In sections E and F, the effect of competition between Cd(II) and Ni(II) in the absence of Pb(II) has been investigated. In the presence of fixed level of Cd(II) and increasing Ni(II), Ni(II) uptake was decreased. A similar result occurred in the F section with the increasing of Cd(II) as well as a fixed level of Ni(II). However, the results showed that the uptake percentage of Cd(II) is higher than Ni(II) uptake in all of the experimental sections. These results showed

Table 5 Comparison of single, binary, and ternary systems

Concentration (mg L^{-1})				Uptake %			
Section	Pb(II)	Cd(II)	Ni(II)	Pb(II)	Cd(II)	Ni(II)	Total
	50	0	0	96.19 ± 2.1	0	0	96.19
	50	50	0	95.91 ± 5.4	76.22 ± 5.7	0	86.06
	50	100	0	94.99 ± 4.5	73.50 ± 0.8	0	84.24
A	50	150	0	94.35 ± 7.2	68.34 ± 3.2	0	81.34
	50	200	0	93.79 ± 0.9	60.96 ± 1.1	0	77.37
	50	250	0	91.22 ± 3.7	43.84 ± 4.8	0	67.53
	50	300	0	80.99 ± 7.8	22.00 ± 0.9	0	51.49
	50	0	0	96.19 ± 2.1	0	0	96.19
	50	0	50	98.73 ± 4.7	0	35.63 ± 0.6	67.18
	50	0	100	97.51 ± 7.2	0	28.64 ± 0.9	63.07
B	50	0	150	97.10 ± 7.8	0	20.18 ± 0.5	58.64
	50	0	200	96.86 ± 5.5	0	18.42 ± 0.6	57.64
	50	0	250	95.97 ± 3.7	0	12.15 ± 0.4	54.06
	50	0	300	95.51 ± 4.6	0	10.80 ± 1.2	53.15
	0	50	0	0	80.00 ± 1.5	0	80.00
	50	50	0	95.91 ± 5.4	76.22 ± 5.7	0	86.06
	100	50	0	91.32 ± 6.1	69.26 ± 3.5	0	80.29
C	150	50	0	88.92 ± 4.4	60.45 ± 1.8	0	74.68
	200	50	0	84.34 ± 7.2	55.67 ± 1.1	0	70.00
	250	50	0	81.44 ± 6.2	49.92 ± 4.1	0	65.68
	300	50	0	78.51 ± 3.1	35.64 ± 1.1	0	57.07
	0	0	50	0	0	55.88 ± 1.2	55.88
	50	0	50	98.73 ± 4.7	0	35.63 ± 0.6	67.18
	100	0	50	95.32 ± 2.3	0	28.43 ± 0.8	61.87
D	150	0	50	91.92 ± 1.1	0	19.91 ± 1.5	55.91
	200	0	50	87.34 ± 2.1	0	17.11 ± 1.3	52.22
	250	0	50	85.44 ± 1.8	0	12.10 ± 0.5	48.77
	300	0	50	80.51 ± 2.7	0	10.60 ± 0.6	45.55
	0	50	0	0	80.00 ± 1.5	0	80.00
	0	50	50	0	78.25 ± 5.6	52.75 ± 1.5	65.50
	0	50	100	0	62.16 ± 0.7	49.10 ± 0.9	55.63
E	0	50	150	0	51.84 ± 2.4	44.97 ± 0.6	48.40
	0	50	200	0	45.20 ± 2.8	38.83 ± 1.4	42.01
	0	50	250	0	31.13 ± 1.2	24.90 ± 0.4	28.01
	0	50	300	0	28.96 ± 2.3	9.30 ± 0.3	19.13
	0	0	50	0	0	55.88 ± 1.2	55.88
	0	50	50	0	78.25 ± 5.6	52.75 ± 1.5	65.50
	0	100	50	0	71.26 ± 5.5	48.15 ± 2.5	59.70
F	0	150	50	0	66.88 ± 0.3	35.12 ± 0.9	51.00
	0	200	50	0	57.41 ± 3.8	27.45 ± 2.2	42.43
	0	250	50	0	43.76 ± 2.4	18.34 ± 1.4	31.05
	0	300	50	0	16.40 ± 1.3	12.15 ± 0.4	14.27
	50	0	0	96.19 ± 2.1	0	0	96.19
	50	50	50	95.93 ± 3.1	69.06 ± 1.2	28.15 ± 2.5	64.38
	50	100	100	90.07 ± 5.5	64.68 ± 3.4	24.56 ± 1.5	59.77

Table 5 (continued)

Concentration (mg L^{-1})				Uptake %			
Section	Pb(II)	Cd(II)	Ni(II)	Pb(II)	Cd(II)	Ni(II)	Total
G	50	150	150	86.01 ± 4.3	57.75 ± 2.5	18.69 ± 2.1	54.15
	50	200	200	79.91 ± 4.5	47.73 ± 1.5	14.56 ± 0.8	47.40
	50	250	250	67.84 ± 2.5	26.55 ± 2.3	10.12 ± 0.5	34.83
	50	300	300	61.73 ± 2.8	19.12 ± 0.5	8.50 ± 0.4	29.78

higher selectivity of *D. salina* for Cd(II) than that for Ni(II). In the last part of the simultaneous biosorption (G), Pb(II) uptake in the presence of competitive ions, Cd(II) and Ni(II) internary systems were investigated. The concentration of Pb(II) was fixed, and the concentration of Cd(II) and Ni(II) increased simultaneously. It can be seen that Pb(II) uptake (96.19–61.73%) is higher than Cd(II) uptake (69.06–19.12%) and Ni(II) uptake (28.15–8.5%) in ternary systems.

It may be due to the possible interaction between various types of metal ions and *D. salina* cell wall as a dynamic sorbent in biosorption systems. Essential factors of biosorption may affect the binding site properties such as surface structure, functional groups, ionic size, ionic charge, ionic weight (the weight of an ion as determined by the sum of the atomic weights of its components), heavy metal ion concentration, standard redox potential of the metal ions, ionic strength, and pH. Therefore, it is difficult to explain which common parameters have more influence on the interaction mechanism and selectivity of biosorption in a mixed heavy metal ion system (Verma et al., 2021).

Multicomponent equilibrium isotherms

For the investigation of multicomponent effects on Cd(II), Ni(II), and Pb(II), it is important to know the biosorption isotherm. Two major mathematical isotherm models, namely, Langmuir and Freundlich, described the distribution of the sorbent surface between *D. salina* and liquid phases. The Langmuir isotherm is the widest model that assumes homogeneous adsorption and monolayer coverage on the sorbent with no interaction between the adsorbed ions or molecules. The linearized Langmuir model is expressed in Eq. (6) (Guo & Wang, 2019; Li et al., 2011):

$$\frac{C_e}{q_e} = \frac{1}{q_m b} + \frac{C_e}{q_m} \tag{6}$$

where q_e is the adsorbed value of competitive heavy metal ions at equilibrium concentration (mg g^{-1}) on the surface of *D. salina*,C_e is the equilibrium concentration of competitive heavy metal ions (mg L^{-1}),q_m is the maximum adsorption capacity on adsorbent (mg g^{-1}), and b represents the Langmuir constant related to affinity of heavy metal ions on the *D. salina* and the adsorption energy (L mg^{-1}) (Malik et al., 2018).

The Freundlich isotherm, unlike the Langmuir isotherm, is considered multilayer adsorption at the surface of *D. salina* and heterogeneous adsorption as following Eq. (7):

$$log\ q_e = log\ k_f + \frac{1}{n} log\ C_e \tag{7}$$

The values of Freundlich constants include n, the heterogeneity parameter, related to biosorption intensity of heavy metal ions on the *D. salina*, and k_f (mg g^{-1}) indicates the maximum biosorption capacity of heavy metal ions. For binary and ternary systems, Langmuir and Freundlich isotherms were applied to determine the effect of another heavy metal ion on the linear regression coefficients and isotherm constants.

In Table 6, the isotherm constant values for (Pb–Cd), (Pb–Ni), (Cd–Ni), and (Pb–Cd–Ni) ions are listed. For (Pb–Cd) and (Pb–Ni) systems, when Pb(II) is the competitive ion, the isotherms best fit with Freundlich isotherm (0.9980 and 0.9969). For Cd(II) as a competitive ion, in the (Pb–Cd) and (Cd–Ni) systems, the isotherms best fit with Langmuir under the R^2 values of 0.9644 and 0.9825 respectively. Ni(II), as a competitive ion showed, a different pattern in binary systems. In (Pb–Ni) binary systems, better correlation coefficient has shown for the Langmuir isotherm, while in (Cd–Ni) binary systems, the best fit has shown for Freundlich isotherm. Ternary systems (Pb–Cd–Ni) have shown the best fit with Langmuir model for both Cd(II) and Ni(II) as the competitive ions. The applicability of both

Table 6 Biosorption isotherm model constants for binary and ternary systems

Metal(II)	Langmuir			Freundlich		
	b (Lmg^{-1})	q_m (mg g^{-1})	R^2	1/*n*	K_f (mg g^{-1})	R^2
Pb (Pb-Cd)	0.06	476.19	0.9712	0.46	57.46	0.9980
Pb (Pb-Ni)	0.17	384.61	0.9725	0.36	94.78	0.9969
Cd (Pb-Cd)	0.05	217.39	0.9644	0.45	25.16	0.8270
Cd (Cd-Ni)	0.05	217.39	0.9825	0.43	26.65	0.8898
Ni (Pb-Ni)	0.05	58.82	0.9726	0.27	13.22	0.7269
Ni (Cd-Ni)	0.03	133.33	0.9006	0.68	5.26	0.9876
Cd (Pb-Cd–Ni)	2.18	120.48	0.9304	0.30	31.96	0.5360
Ni (Pb-Cd–Ni)	0.07	46.51	0.9680	0.27	10.57	0.6136

isotherm models implied homogenous biosorption of metal ions on *D. salina*, as well as heterogeneous surface of *D. salina*, for the biosorption of different heavy metal ions (Figs. S1 and S2). Adsorption constants of the isotherms indicated the surface properties and affinity of the functional groups for heavy metal ions. These parameters can be used to compare the biosorption capacity of *D. salina* algae for selected heavy metal ions in the binary and ternary systems. All binary and ternary systems show that their q_m and K_f parameters for Langmuir and Frendlich models decrease according to the following category: Pb(II) > Cd(II) > Ni(II).

Heayy metal ion removal from real water

To further explore the actual applicability of the *D. salina* for simultaneous heavy metal ion biosorption in a broader context, real water was used. The percentage removal was calculated and shown in Table 7. This fact clearly indicates the affinity of *D. salina* for Pb(II) ion uptake even in the presence of Cd(II) and Ni(II) and other compounds existing in real water.

In conclusion, Table 8 shows the various algal species for heavy metal ion removal and other parameters in the literature. It can be noteworthy that the removal of *D. salina* and simultaneous uptake for Pb(II) are higher than those of Cd(II) and Ni(II) in real samples.

FT- IR analysis

FT- IR spectra before and after heavy metal ion uptake were recorded to identify the functional groups on the *D. salina* surface. The FT-IR spectra are shown in Fig. 3 for the *D. salina* surface in four different forms: the *D. salina* algae before biosorption, and after biosorption of Pb(II), Cd(II), and Ni(II). As shown in Fig. 3, some functional group bands have shifted in the biosorption process indicating the involvement in binding to heavy metal ions and *D. salina* surface. The broad band observed between 3700 and 3200 cm^{-1} is attributed to the O–H symmetric stretching vibration and amine groups on the cell wall of algae (Elleuch et al., 2021). The peaks at 2925 cm^{-1} and in the area around 1400 cm^{-1} were detected in all spectra and can be ascribed to the methyl groups stretching vibrations of aliphatic groups on the microalgae cell wall (Reza et al., 2019). Also, the peak at around 1648–1650 cm^{-1} reflects the presence of C = O of amide groups due to the presence of proteins on the cell wall of *D. salina* (Sulaymon et al., 2013). The peaks at 1410–1420 cm^{-1} could be assigned to COO^- of the carboxylate groups (Farinella et al., 2008).

After heavy metal ion uptake, FT-IR spectrum of Pb(II), Cd(II), and Ni(II) binding on *D. salina* surface has undergone changes and shifts in intensity and wave

Table 7 Biosorption of Pb(II), Cd(II), and Ni(II) by *D. salina* from real waters

Sample	M(II) (mg L^{-1})			Removal %		
	Pb(II)	Cd(II)	Ni(II)	Pb(II)	Cd(II)	Ni(II)
Caspian Sea	50	50	50	90.63 ± 7.8	72.28 ± 3.6	30.80 ± 2.5
well water	50	50	50	93.80 ± 4.1	75.42 ± 4.2	35.68 ± 3.4

Table 8 Comparison of heavy metal ion removal by different algae species

Species of algae	M^{n+}	C_0 (mg L^{-1})	pH	Removal %	Ref.
Scenedesmus quadricauda	Pb(II) Cd(II)	10	5	82 66	(Mirghaffari et al., 2015)
Kappaphycus striatum	Pb(II) Cd(II)	50 50	5	97.82 75.74	(Verma et al., 2021)
Phormidium sp.	Pb(II)	10	5	92.2	(Das et al., 2015)
Ascophyllum nodosum	Pb(II)	50	3	-	(Romera et al., 2007)
Dunaliella salina	Pb(II) Cd(II) Ni(II)	50 50 50	6	90.63 72.28 30.80	This work, Caspian Sea
Dunaliella salina	Pb(II) Cd(II) Ni(II)	50 50 50	6	93.80 75.42 35.68	This work, well water

number of some peaks (Fig. 3). The shifted peak of hydroxyl group at the cell wall of *D. salina* indicates the complex formation between these -OH groups with heavy metal ions. Furthermore, the peak at 1411 cm^{-1} that shifted to the maximum of 1419 cm^{-1} shows binding of heavy metal ions to COO^-functional group in the biosorption process. Green microalgae are composed of many carboxyl groups that are responsible for metal ion biosorption. In addition, peak at around 1648 $cm^{-1}$was observed to shift to 1652–1655 cm^{-1} in all samples, indicating interaction of heavy metal ions with carboxylic groups of proteins for amide component.

As a result, the functional groups including hydroxyl, carboxyl, and amide compounds are responsible for the biosorption of heavy metal ions (Ziaei et al. 2022). Moreover, it was found that the *D. salina* algae could be efficient biosorbent due to the presence of functional groups participating in the biosorption process (Reza et al., 2019).

Characterization of *D. salina*

The morphological characterization and elemental analysis of the *D. salina* surface before and after biosorption of heavy metal ions were obtained by SEM and EDX

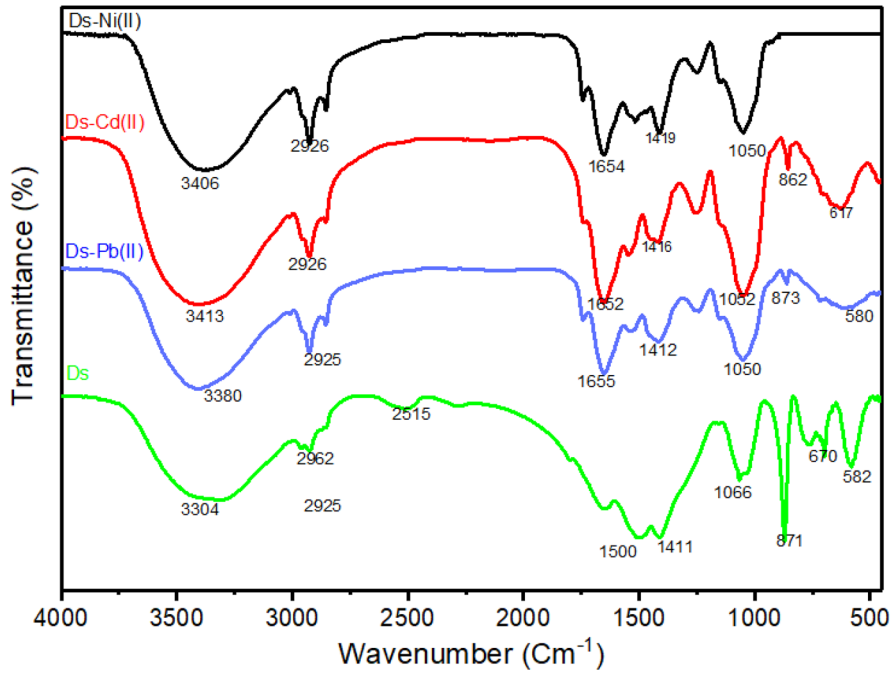

Fig. 3 FT-IR spectra of the *D. salina* after and before Pb(II), Cd(II), and Ni(II) uptake

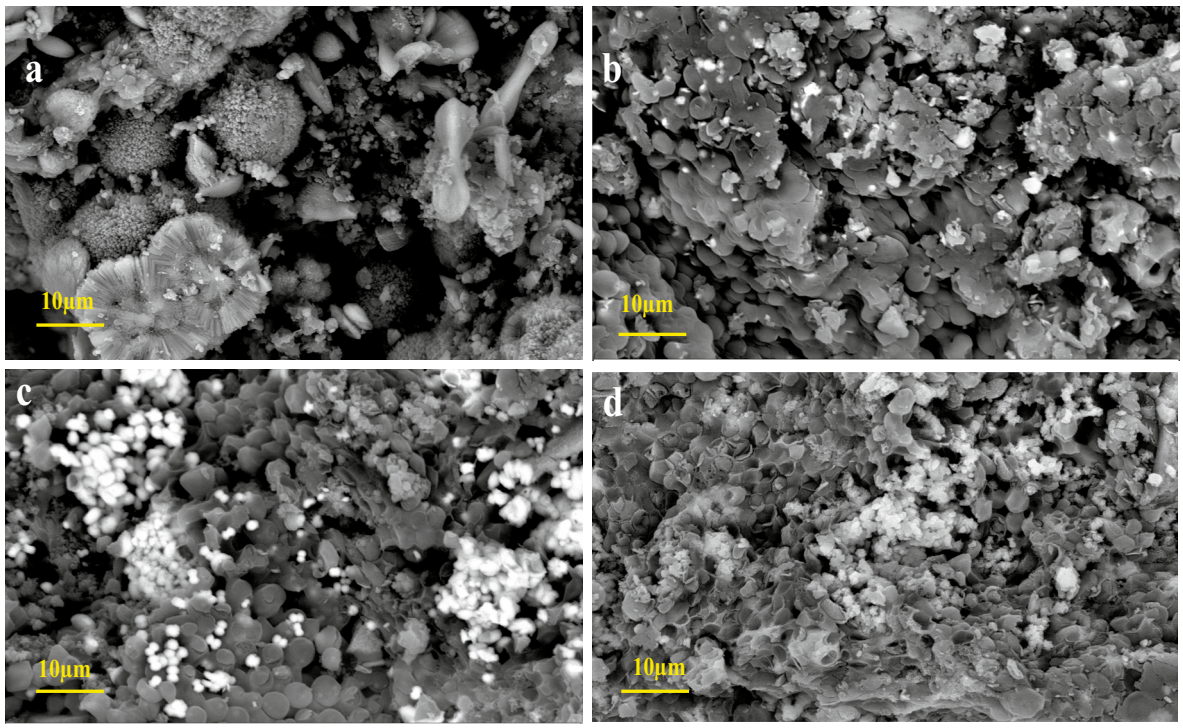

Fig. 4 SEM images before uptake of heavy metal ions by *D. salina* (**a**) and after uptake of Pb(II) (**b**), Cd(II) (**c**), and Ni(II) (**d**)

techniques. The SEM image in Fig. 4a indicates a rough and irregular surface with porous texture of *D. salina* as a control sample that provides the interaction with heavy metal ions in aqua solution. In contrast, Fig. 4b–d show *D. salina* surface with considerable differences after biosorption of Pb(II), Cd(II), and Ni(II). These significant differences indicate the biosorption of heavy metal ions on *D. salina* cell wall (Verma et al., 2021).

EDX spectra of elemental analysis for *D. salina* cell wall before and after biosorption of heavy metal ions are also shown in Fig. 5. Heavy metal ions were not found before the biosorption (Fig. 5a); but after biosorption, the peaks of Pb(II), Cd(II), and Ni(II) on the biomass are strong evidence of biosorption by *D. salina* cell wall (Fig. 5a–c). Similar study was reported to remove Cr(III) by *D. salina* (Kaushik & Raza, 2019).

Biosorption selectivity

For adsorption processes, selectivity is a parameter highly related to qualitative analysis. Functional groups play an important role in ion selectivity studies (Awual et al., 2020). In this work, the effect of competing metal ions on the biosorption process of Pb(II) was evaluated. These competing metal ions were chosen from the list of metal ions presented in wastewater. For example, Al(III), Cd(II), Co(II), Cr(III), Cu(II), Mn(II), and Ni(II), were simultaneously presented in a solution containing Pb(II) ions and their effect on the biosorption process were evaluated and shown in Fig. 6. The biosorption efficiency in the presence of selected metal ions demonstrated higher biosorption of Pb(II). The biosorption efficiency was 80% for Pb(II) as compared to Cr (III) (72.26%) due to competitive effect. In this experiment, the foreign metal ion concentrations were tenfold higher than those of the Pb(II). However, the simultaneous removal of these two ions can be important because of multiple heavy metal ions in wastewaters.

Biosorption mechanisms

The process of Pb(II) uptake in living *D. salina* is more complicated as compared to non-living *D. salina*. Biosorption process occurring in the growth process involves both extracellular and intracellular Pb(II) uptake. The first mechanism, fast inactive biosorption,

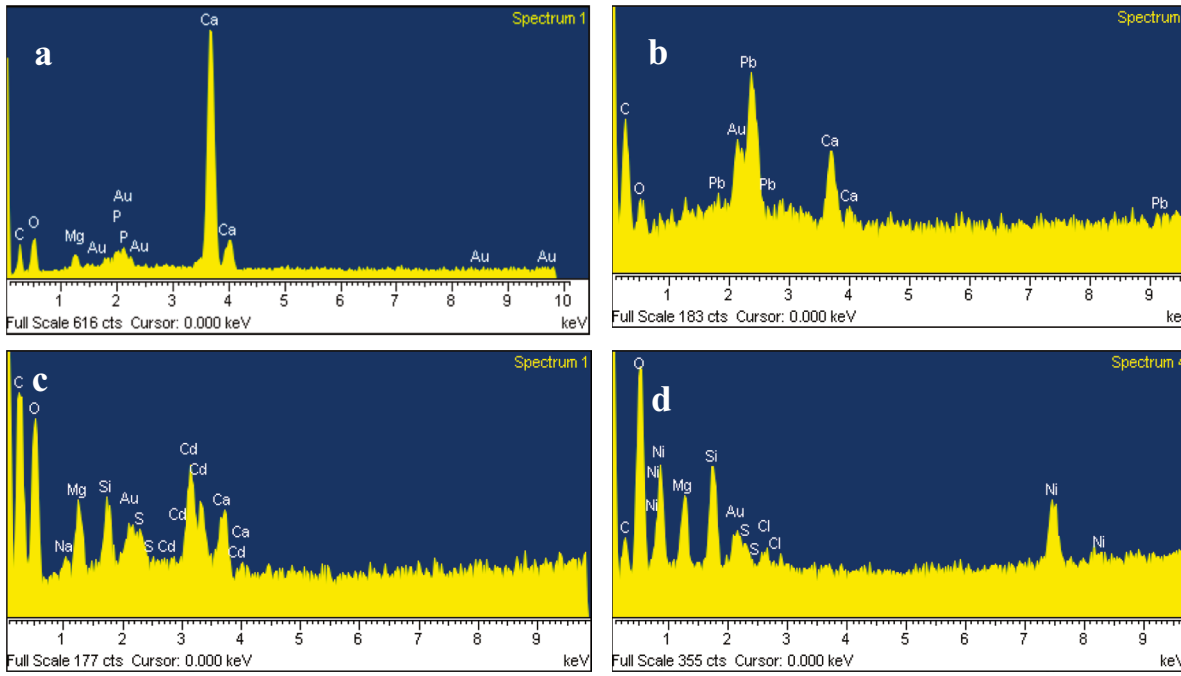

Fig. 5 EDX spectra of *D. salina* before (**a**) and after Pb(II) (**b**), Cd(II), (**c**) and Ni(II) (**d**) uptake

proceeds on the cell surface with mechanisms such as cation exchange, covalent band, physical adsorption, and complex formation with various functional groups on the surface of sorbent. For the second mechanism, slow active biosorption occurs and involves intercellular ion accumulation into the cell cytoplasm (Priya et al., 2022). Figure 7 shows possible mechanisms of heavy metal ion removal by *D. salina.*

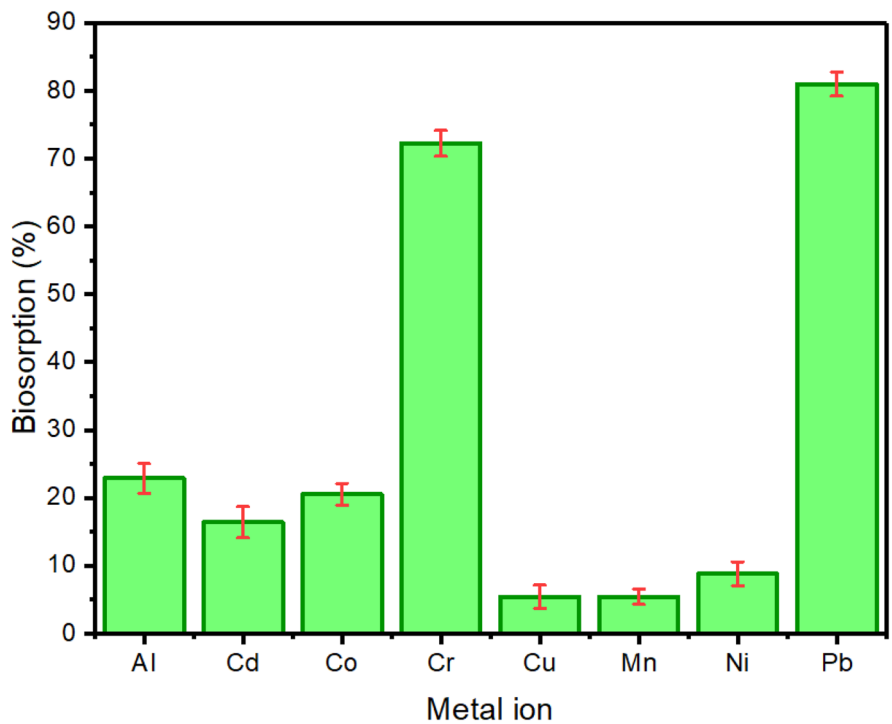

Fig. 6 Competing metal ion effects on Pb(II) biosorption (Pb(II) concentration:10 mg L^{-1}, competing ion concentration:100 mg L^{-1})

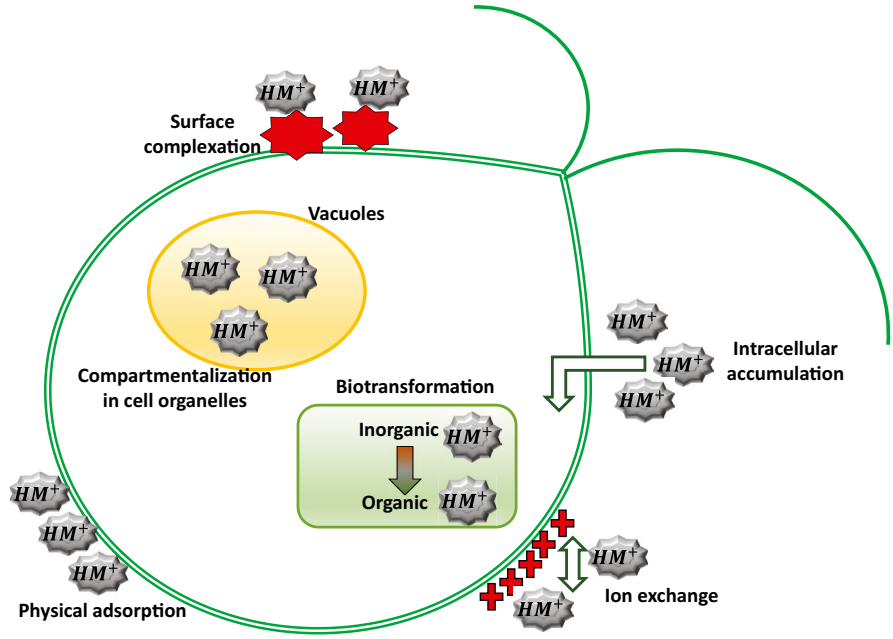

Fig. 7 Possible mechanisms of heavy metal ion removal by *D. salina*

The growth cycle of *D. salina* is a dynamic process, and the criteria of OD is not valid to differentiate between live *D. salina* generated in the growth media and the *D. salina* after the adsorption of Pb(II) on its surface to understand whether it is live or inactivated. Because the study is performed on a laboratory scale, the regeneration of *D. salina* was not taken into consideration. On a large scale, the recovery of Pb(II) ions is usually performed by anaerobic digesting of biomass to produce methane gas and collecting the heavy metals from the digester. It may be interesting to do cost–benefit analysis of regenerating *D. salina* process after adsorption or production of fresh *D. salina* due to natural growth.

Conclusion

Herein, we suggest to use *D. salina* as an economic biosorbent that provides continuous and effective Pb(II) uptake. The morphology and structure properties of *D. salina* were characterized by SEM, EDX, and FT-IR. The influence of vital parameters, including pH, OD of microalgae, contact time, injection time, and Pb(II) concentration was successfully modeled and optimized by RSM-CCD method. The results of this study illustrated that the Pb(II) uptake is strongly influenced by pH and Pb(II) concentration. The Pb(II) uptake efficiency was 96% under optimum RSM conditions. Biosorption of Cd(II), Ni(II), and Pb(II) has been investigated for single, binary, and ternary systems. The biosorption capacity is highest for Pb(II) as compared to Cd(II) and Ni(II) for all systems. Competitive isotherm models indicated that Pb(II) follows the Freundlich isotherm, while the Langmuir isotherm is governed by Cd(II). Additionally, Ni(II) follows both Langmuir and Freundlich isotherms in the presence of Pb(II) and Cd(II). Moreover, *D. salina* revealed impressive biosorption of Pb(II) (80%) in the presence of ten times higher concentrations of commonly available heavy metal ions in wastewater.

In the present study, *D. salina* was directly grown in saline water and used to treat heavy metal ions from contaminated waters. This is a feasible solution to environmental problems. Research findings led to the recommendation of a novel model for using live microalgae as an eco-friendly and green approach that avoids the usage of any chemicals that may impose serious damage to the environment. More notably, these results might be scaled up using live *D. Salina* to establish cost-effectiveness biosorption for the bioremediation of heavy metal ion contaminations in wastewater.

Acknowledgements As authors of the article, we acknowledge Ferdowsi University of Mashhad for supporting this project (grant number: 3/51645).

Author contribution Somayyeh Ziaei: data collection, sample analysis, writing (original draft), and data interpretation. Hossein Ahmadzadeh: conceptualization, data analysis, funding acquisition, project supervision, and data validation. Zarrin Es'haghi: conceptualization, data analysis, and writing (review and editing).

Funding This study is funded by Ferdowsi University of Mashhad (grant number: 3/51645).

Data availability The datasets generated during the current study are available from the corresponding author upon reasonable request.

Declarations

Competing interests The authors declare no competing interests.

References

Abdel, A. M., Ammar, N. S., Ghafar, H. H. A., & Ali, R. K. (2013). Biosorption of cadmium and lead from aqueous solution by fresh water alga Anabaena sphaerica biomass. *Journal of Advanced Research, 4*(4), 367–374. https://doi.org/10.1016/j.jare.2012.07.004

Anastopoulos, I., & Kyzas, G. Z. (2015). Progress in batch biosorption of heavy metals onto algae. *Journal of Molecular Liquids, 209*, 77–86. https://doi.org/10.1016/j.molliq.2015.05.023

Awual, M. R., Hasan, M. M., Iqbal, J., Islam, A., Islam, M. A., Asiri, A. M., & Rahman, M. M. (2020). Naked-eye lead(II) capturing from contaminated water using innovative large-pore facial composite materials. *Microchemical Journal, 154*, 104585–104594. https://doi.org/10.1016/j.microc.2019.104585

Bai, M. T., & Venkateswarlu, P. (2019). Optimization studies for lead biosorption on Sargassum tenerrimum (brown algae) using experimental design : Response surface methodology. *Materials Today: Proceedings, 18*, 4290–4298. https://doi.org/10.1016/j.matpr.2019.07.387

Basu, M., Guha, A. K., & Ray, L. (2017). Adsorption of lead on cucumber peel. *Journal of Cleaner Production, 151*, 603–615. https://doi.org/10.1016/j.jclepro.2017.03.028

Belghith, T., Athmouni, K., Bellassoued, K., El Feki, A., & Ayadi, H. (2016). Physiological and biochemical response of Dunaliella salina to cadmium pollution. *Journal of Applied Phycology, 28*(2), 991–999. https://doi.org/10.1007/s10811-015-0630-5

Das, D., Chakraborty, S., Bhattacharjee, C., & Chowdhury, R. (2015). Biosorption of lead ions (Pb2+) from simulated wastewater using residual biomass of microalgae. *New Pub: Balaban, 57*(10), 4576–4586. https://doi.org/10.1080/19443994.2014.994105

Dönmez, G., & Aksu, Z. (2002). Removal of chromium(VI) from saline wastewaters by Dunaliella species. *Process Biochemistry, 38*(5), 751–762. https://doi.org/10.1016/S0032-9592(02)00204-2

Eliescu, A., Georgescu, A. A., Nicolescu, C. M., Bumbac, M., Cioateră, N., Mureșeanu, M., et al. (2020). Biosorption of Pb(II) from aqueous solution using mushroom (Pleurotus ostreatus) biomass and spent mushroom substrate. *Analytical Letters, 53*(14), 2292–2319. https://doi.org/10.1080/00032719.2020.1740722

Elleuch, J., Ben Amor, F., Chaaben, Z., Frikha, F., Michaud, P., Fendri, I., et al. (2021). Zinc biosorption by Dunaliella sp. AL-1: Mechanism and effects on cell metabolism. *Science of the Total Environment, 773*, 145024–145038. https://doi.org/10.1016/j.scitotenv.2021.145024

Esposito, A., Pagnanelli, F., & Vegliò, F. (2002). pH-related equilibria models for biosorption in single metal systems. *Chemical Engineering Science, 57*(3), 307–313. https://doi.org/10.1016/S0009-2509(01)00399-2

Esvandi, Z., Foroutan, R., Mirjalili, M., Sorial, G. A., & Ramavandi, B. (2019). Physicochemical behavior of Penaeuse semisulcatuse chitin for Pb and Cd removal from aqueous environment. *Journal of Polymers and the Environment, 27*(2), 263–274. https://doi.org/10.1007/s10924-018-1345-x

Farinella, N. V., Matos, G. D., Lehmann, E. L., & Arruda, M. A. Z. (2008). Grape bagasse as an alternative natural adsorbent of cadmium and lead for effluent treatment. *Journal of Hazardous Materials, 154*(1), 1007–1012. https://doi.org/10.1016/j.jhazmat.2007.11.005

Fawzy, M. A., Darwish, H., Alharthi, S., Al-Zaban, M. I., Noureldeen, A., & Hassan, S. H. A. (2022). Process optimization and modeling of Cd2+ biosorption onto the free and immobilized Turbinaria ornata using Box-Behnken experimental design. *Scientific Reports, 12*(1), 1–18. https://doi.org/10.1038/s41598-022-07288-z

Fawzy, M. A., & Gomaa, M. (2020). Use of algal biorefinery waste and waste office paper in the development of xerogels: a low cost and eco-friendly biosorbent for the effective removal of congo red and Fe (II) from aqueous solutions. *Journal of Environmental Management*, *262*, 110380. https://doi.org/10.1016/j.jenvman.2020.110380

Fawzy, M. A., Hifney, A. F., Adam, M. S., & Al-Badaani, A. A. (2020). Biosorption of cobalt and its effect on growth and metabolites of Synechocystis pevalekii and Scenedesmus bernardii: isothermal analysis. *Environmental Technology and Innovation*, *19*, 100953. https://doi.org/10.1016/j.eti.2020.100953

Giraldo, L., Guar, J. R., Rodr, P., & Moreno-piraja, J. C. (2019). Simple and competitive adsorption study of nickel (II) and chromium (III) on the surface of the brown algae Durvillaea antarctica biomass. *ACS Omega, 19*, 18147–18158. https://doi.org/10.1021/acsomega.9b02061

Gu, S., Boase, E. M., & Lan, C. Q. (2021). Enhanced Pb (II) removal by green alga Neochloris oleoabundans cultivated in high dissolved inorganic carbon cultures. *Chemical Engineering Journal*, *416*, 128983. https://doi.org/10.1016/j.cej.2021.128983

Gu, S., & Lan, C. Q. (2021). Biosorption of heavy metal ions by green alga Neochloris oleoabundans : effects of metal ion properties and cell wall structure. *Journal of Hazardous*

Materials, *418*, 126336. https://doi.org/10.1016/j.jhazmat.2021.126336

Guo, X., & Wang, J. (2019). Comparison of linearization methods for modeling the Langmuir adsorption isotherm. *Journal of Molecular Liquids, 296*, 111850–111886. https://doi.org/10.1016/j.molliq.2019.111850

Isam, M., Baloo, L., Kutty, S. R. M., & Yavari, S. (2019). Optimisation and modelling of Pb (II) and Cu (II) biosorption onto red algae (Gracilaria changii) by using response surface methodology. *Water, 11*(11), 2325–2343. https://doi.org/10.3390/w11112325

Kamal, B., & Rafey, A. (2021). A mini review of treatment methods for lead removal from wastewater. *International Journal of Environmental Analytical Chemistry*, 1–16. https://doi.org/10.1080/03067319.2021.1934833

Katheresan, V., Kansedo, J., & Lau, S. Y. (2018). Efficiency of various recent wastewater dye removal methods: A review. *Journal of Environmental Chemical Engineering, 6*(4), 4676–4697. https://doi.org/10.1016/j.jece.2018.06.060

Kaushik, G., & Raza, K. (2019). Potential of novel Dunaliella salina from sambhar salt lake, India, for bioremediation of hexavalent chromium from aqueous effluents : An optimized green approach. *Ecotoxicology and Environmental Safety, 180*, 430–438. https://doi.org/10.1016/j.ecoenv.2019.05.039

Kester, D. R., Duedall, I. W., Connors, D. N., & Pytkowicz, R. M. (1967). Preparation of artificial seawater 1. *Limnology and Oceanography, 12*(1), 176–179.

Kit, Y., & Chang, J. (2020). Bioremediation of heavy metals using microalgae : Recent advances and mechanisms. *Bioresource Technology, 303*, 122886–122897. https://doi.org/10.1016/j.biortech.2020.122886

Kumar, R., Bishnoi, N. R., & Garima, & Bishnoi, K. (2008). Biosorption of chromium(VI) from aqueous solution and electroplating wastewater using fungal biomass. *Chemical Engineering Journal, 135*(3), 202–208. https://doi.org/10.1016/j.cej.2007.03.004

Lee, Y., & Chang, S. (2011). The biosorption of heavy metals from aqueous solution by Spirogyra and Cladophora filamentous macroalgae. *Bioresource Technology, 102*(9), 5297–5304. https://doi.org/10.1016/j.biortech.2010.12.103

Li, Y., Zhang, P., Du, Q., Peng, X., Liu, T., Wang, Z., et al. (2011). Adsorption of fluoride from aqueous solution by graphene. *Journal of Colloid and Interface Science, 363*(1), 348–354. https://doi.org/10.1016/j.jcis.2011.07.032

Malik, H., Qureshi, U. A., Muqeet, M., Mahar, R. B., Ahmed, F., & Khatri, Z. (2018). Removal of lead from aqueous solution using polyacrylonitrile/magnetite nanofibers. *Environmental Science and Pollution Research, 25*(4), 3557–3564. https://doi.org/10.1007/s11356-017-0706-7

Mirghaffari, N., Moeini, E., & Farhadian, O. (2015). Biosorption of Cd and Pb ions from aqueous solutions by biomass of the green microalga, Scenedesmus quadricauda. *Journal of Applied Phycology, 27*(1), 311–320. https://doi.org/10.1007/s10811-014-0345-z

Mohd Udaiyappan, A. F., Abu Hasan, H., Takriff, M. S., & Sheikh Abdullah, S. R. (2017). A review of the potentials, challenges and current status of microalgae biomass applications in industrial wastewater treatment. *Journal of Water Process Engineering, 20*, 8–21. https://doi.org/10.1016/j.jwpe.2017.09.006

Morosanu, I., Teodosiu, C., Paduraru, C., Ibanescu, D., & Tofan, L. (2017). Biosorption of lead ions from aqueous ef fl uents by rapeseed biomass. *New Biotechnology, 39*, 110–124. https://doi.org/10.1016/j.nbt.2016.08.002

Mosleh, S., Rahimi, M. R., Ghaedi, M., Dashtian, K., & Hajati, S. (2018). Sonochemical-assisted synthesis of CuO/Cu2O/Cu nanoparticles as efficient photocatalyst for simultaneous degradation of pollutant dyes in rotating packed bed reactor: LED illumination and central composite design optimization. *Ultrasonics Sonochemistry, 40*, 601–610. https://doi.org/10.1016/j.ultsonch.2017.08.007

Naveed, S., Li, C., Lu, X., Chen, S., Yin, B., Zhang, C., & Ge, Y. (2019). Microalgal extracellular polymeric substances and their interactions with metal(loid)s: A review. *Critical Reviews in Environmental Science and Technology, 49*(19), 1769–1802. https://doi.org/10.1080/10643389.2019.1583052

Plazinski, W. (2013). Binding of heavy metals by algal biosorbents. Theoretical models of kinetics, equilibria and thermodynamics. *Advances in Colloid and Interface Science, 197–198*, 58–67. https://doi.org/10.1016/j.cis.2013.04.002

Priya, A. K., Jalil, A. A., Vadivel, S., Dutta, K., Rajendran, S., Fujii, M., & Soto-Moscoso, M. (2022). Heavy metal remediation from wastewater using microalgae: recent advances and future trends. *Chemosphere*, *305*, 135375. https://doi.org/10.1016/j.chemosphere.2022.135375

Pugazhendhi, A., Boovaragamoorthy, G. M., Ranganathan, K., Naushad, M., & Kaliannan, T. (2018). New insight into effective biosorption of lead from aqueous solution using Ralstonia solanacearum: Characterization and mechanism studies. *Journal of Cleaner Production, 174*, 1234–1239. https://doi.org/10.1016/j.jclepro.2017.11.061

Qin, H., Hu, T., Zhai, Y., Lu, N., & Aliyeva, J. (2020). The improved methods of heavy metals removal by biosorbents: A review. *Environmental Pollution, 258*, 113777–113841. https://doi.org/10.1016/j.envpol.2019.113777

Reza, A., Ali, M., Sohbatzadeh, H., & Mofras, M. (2019). Groundwater for sustainable development La (III) and Ce (III) biosorption on sulfur functionalized marine brown algae Cystoseira indica by xanthation method : Response surface methodology, isotherm and kinetic study. *Groundwater for Sustainable Development, 8*, 144–155. https://doi.org/10.1016/j.gsd.2018.10.005

Romera, E., González, F., Ballester, A., Blázquez, M. L., & Muñoz, J. A. (2007). Comparative study of biosorption of heavy metals using different types of algae. *Bioresource Technology, 98*(17), 3344–3353. https://doi.org/10.1016/j.biortech.2006.09.026

Shen, Z., Hou, D., Jin, F., Shi, J., Fan, X., Tsang, D. C. W., & Alessi, D. S. (2019). Effect of production temperature on lead removal mechanisms by rice straw biochars. *Science of the Total Environment, 655*, 751–758. https://doi.org/10.1016/j.scitotenv.2018.11.282

Sohbatzadeh, H., Keshtkar, A. R., Safdari, J., & Fatemi, F. (2016). U(VI) biosorption by bi-functionalized Pseudomonas putida @ chitosan bead: Modeling and optimization using RSM. *International Journal of Biological Macromolecules, 89*, 647–658. https://doi.org/10.1016/j.ijbiomac.2016.05.017

Sulaymon, A. H., Mohammed, A. A., & Al-musawi, T. J. (2013). Competitive biosorption of lead, cadmium, copper, and arsenic ions using algae. *Environmental Science and*

Pollution Research, 20(5), 3011–3023. https://doi.org/10.1007/s11356-012-1208-2

Suresh Kumar, K., Dahms, H. U., Won, E. J., Lee, J. S., & Shin, K. H. (2015). Microalgae - a promising tool for heavy metal remediation. *Ecotoxicology and Environmental Safety, 113*, 329–352. https://doi.org/10.1016/j.ecoenv.2014.12.019

Turkmen Koc, S. N., Kipcak, A. S., Moroydor Derun, E., & Tugrul, N. (2020). Removal of zinc from wastewater using orange, pineapple and pomegranate peels. *International Journal of Environmental Science and Technology, 18*(9), 2781–2792. https://doi.org/10.1007/s13762-020-03025-z

Verma, A., Agarwal, M., Sharma, S., & Singh, N. (2021). Competitive removal of cadmium and lead ions from synthetic wastewater using Kappaphycus striatum. *Environmental Nanotechnology, Monitoring & Management, 15*, 100449–100460. https://doi.org/10.1016/j.enmm.2021.100449

Vidyalaxmi, Kaushik, G., & Raza, K. (2019). Potential of novel Dunaliella salina from sambhar salt lake, India, for bioremediation of hexavalent chromium from aqueous effluents: an optimized green approach. *Ecotoxicology and Environmental Safety*, *180*, 430–438. https://doi.org/10.1016/j.ecoenv.2019.05.039

Wang, J., & Chen, C. (2009). Biosorbents for heavy metals removal and their future. *Biotechnology Advances, 27*(2), 195–226. https://doi.org/10.1016/j.biotechadv.2008.11.002

Wang, Y., Zhang, C., Zheng, Y., & Ge, Y. (2017). Bioaccumulation kinetics of arsenite and arsenate in Dunaliella salina under different phosphate regimes. *Environmental Science and Pollution Research, 24*(26), 21213–21221. https://doi.org/10.1007/s11356-017-9758-y

Wei, J. J., Duan, L., Wei, J. J., Hoffmann, E., Song, Y., & Meng, X. (2021). Lead removal from water using organic acrylic amine fiber (AAF) and inorganic-organic P-AAF, fixed bed filtration and surface-induced precipitation. *Journal of Environmental Sciences, 101*, 135–144. https://doi.org/10.1016/j.jes.2020.08.009

Yan, C., Qu, Z., Wang, J., Cao, L., & Han, Q. (2022). Microalgal bioremediation of heavy metal pollution in water : Recent advances, challenges, and prospects. *Chemosphere, 286*(P3), 131870–131883. https://doi.org/10.1016/j.chemosphere.2021.131870

Zeraatkar, A. K., Ahmadzadeh, H., Talebi, A. F., Moheimani, N. R., & McHenry, M. P. (2016). Potential use of algae for heavy metal bioremediation, a critical review. *Journal of Environmental Management, 181*, 817–831. https://doi.org/10.1016/j.jenvman.2016.06.059

Zhang, J., Wei, S., Liu, Z., Tang, H., Meng, X., & Zhu, W. (2022). Release of Pb adsorbed on graphene oxide surfaces under conditions of Shewanella putrefaciens metabolism. *Journal of Environmental Sciences, 118*, 67–75. https://doi.org/10.1016/j.jes.2021.08.041

Zhang, Q., Zhang, S., Zhao, Z., Liu, M., Yin, X., Zhou, Y., et al. (2020). Highly effective lead (II) removal by sustainable alkaline activated b - lactoglobulin nano fi brils from whey protein. *255*, 120297. https://doi.org/10.1016/j.jclepro.2020.120297

Ziaei, S., Ahmadzadeh, H., & Es'haghi, Z. (2022). Artemia cysts as dynamic biosorbent for efficient and fast uptake of lead ions from contaminated environments. *International Journal of Environmental Science and Technology, 19*, 6467–6480. https://doi.org/10.1007/S13762-021-03844-8